Original
ISSN 2413-0516

Assessment of Common Clinical Detectors Feasibility for Measuring Small-Field Output Factors in Stereotactic Radiosurgery using Eclipse TPS

Ibrahim H. Alnidawi[1,2*], Haydar H. Alabedi[3], Hany M. Ammar[4], Hassan Abouelenein[5], Atallah Elhanbaly[1], Ahmed Elgarayhi[1], Mohammed Sallah[6]

[1]Physics Department, Faculty of Science, Mansoura University, Mansoura 35516, Egypt.
[2]Department of Radiation Oncology, Warith International Cancer Institute (WICI), Al-Thaqalayne Cancer Hospital, Basra, Iraq.
[3]Department of Medical Oncology, Faculty of Medicine, Baghdad University, Baghdad, Iraq.
[4]Clinical Oncology Department, Faculty of Medicine, Aswan University, Aswan, Egypt.
[5]Minia Oncology Centre, Minia, Egypt.
[6]Department of Physics, College of Sciences, University of Bisha, P.O. Box 344, Bisha 61922, Saudi Arabia.
*Correspondence to: Ibrahim H. Alnidawi (E-mail: ibrahimalnidawi6@gmail.com)
(Submitted: 01 April 2025 – Revised version received: 13 April 2025 – Accepted: 05 May 2025 – Published online: 26 June 2025)

Abstract

Objective: This study aimed to evaluate the comparative suitability of four widely available radiation detectors: the CC13 ionization chamber, Matrixx Evolution, Electronic Portal Imaging Device (EPID), and IBA DQA, for small-field output factor measurements, using the CC01 ionization chamber as the reference standard.

Methods: The output factors were measured for asymmetric field sizes ranging from 1×1 cm^2 to 10×10 cm^2. The collected OF data for each detector was then used to independently configure five separate beam models in the Eclipse TPS (version 17.0), ensuring that all other configuration parameters, such as the PDDs and profiles, remained constant. To assess the clinical impact of the differences in detector-based beam modeling, a retrospective cohort of 20 patient SRS treatment plans was recalculated using each of the five beam models. Comparative dosimetric analyses focused on dose-volume histogram parameters for planning target volumes, organs at risk, high- and intermediate-dose spillage, and total number of monitor units.

Results: The results showed high consistency across all beam models, with no statistically significant differences observed between the CC01-based configuration and those derived from alternative detectors. Deviations in all dosimetric and treatment delivery parameters were minimal and clinically acceptable, indicating a negligible impact on treatment delivery.

Conclusion: These findings suggest that despite the known limitations in small-field dosimetry, the CC13, Matrixx Evolution, EPID, and IBA DQA detectors can reliably derive output factors for TPS commissioning in the SRS context. This provides flexibility in detector selection, particularly in clinics, where access to CC01 may be limited. The dosimetric equivalence demonstrated supports their integration into the clinical workflow for small-field radiotherapy applications.

Keywords: CC01, CC13, matrixx evolution, IBA DQA, eclipse TPS, stereotactic radiosurgery

Introduction

Accurate dose delivery is crucial in modern radiotherapy, especially with the growing use of highly conformal techniques like stereotactic radiosurgery (SRS), stereotactic body radiotherapy (SBRT), and intensity-modulated radiotherapy (IMRT), which frequently utilize small radiation fields. These small fields, typically defined as those with dimensions less than 3×3 cm^2, present unique dosimetric challenges due to the absence of lateral charged particle equilibrium, volume-averaging effects, and detector perturbations. These challenges have spurred significant research efforts and clinical guidance, including the IAEA TRS-483 Code of Practice and AAPM Task Group 155 recommendations.[1,2]

Precise measurement of output factors is essential in small-field dosimetry because these values are primary inputs for configuring treatment planning systems (TPS), such as Eclipse. According to AAPM Task Group 155 and IAEA TRS-483 recommendations, detectors used in small-field measurements must have high spatial resolution and minimal perturbation effects. Chamber detectors like Razor (CC01) are widely accepted as reference tools for such applications due to their small active volume and water-equivalent response. However, these detectors are not always readily available in all clinical settings. They serve as a reference in many TPSs, including Eclipse, where their output factor data are often preconfigured for commissioning.[3,4]

Various detectors have been used for small-field dosimetry, each with its own advantages and disadvantages. Both IBA CC01 and CC13 detectors experience errors and inaccuracies in high-dose gradient areas, which are characteristic of SRS. CC13 chambers were designed specifically for these applications. CC01, with its small volume (0.01 cm^3), effectively reduces volume averaging effects and aligns more closely with calculated dose profiles compared to the larger CC13. However, correction factors are necessary to account for the potential perturbations. In contrast, the CC13 chamber tended to overestimate the dose in the penumbral regions while underestimating the output factors in small fields, primarily because of their larger volume. In comparative studies, alternative detectors, such as plastic scintillation detectors (e.g., Exradin W1) and micro diamond detectors, have demonstrated superior performance, exhibiting excellent concordance with Monte Carlo simulations. This was attributed to their minimal perturbation effects and improved water equivalence, enabling them to serve as reference measurements for benchmarking the performance of CC01 and CC13 under stereotactic conditions.[5–12]

Nevertheless, Razor chambers are not always accessible in all clinical settings due to cost, fragility, and procurement limitations. In contrast, detectors such as the CC13 ionization chamber, Matrixx Evolution 2D array, Electronic Portal Imaging Devices (EPID), and IBA DailyQA (DQA) tools are more commonly integrated into the clinical workflow and are

often used for routine quality assurance (QA). While these tools are convenient and easy to use, their suitability for precise small-field dosimetry and output factor measurement remains under scrutiny. The volume averaging effect, lack of energy-dependence correction, and geometry-related artifacts can lead to systematic errors when these detectors are used outside their recommended clinical applications.[13,14]

Previous studies have compared these detectors for relative dosimetry and QA purposes, but there is a notable gap in research evaluating their feasibility for directly substituting chamber detectors in output factor measurement, particularly when percent depth doses (PDDs) and beam profiles remain constant in the TPS configuration. This study aims to fill this gap by evaluating the dosimetric behavior of the CC13, Matrixx Evolution, EPID, and DQA detectors relative to CC01.[7,8] The goal was to determine their suitability for configuring the output factors within the Eclipse TPS for small-field applications. Therefore, this study investigates whether commonly available detectors such as CC13, Matrixx Evolution, EPID, and DQA can provide clinically acceptable output factor measurements for small fields ($\leq 10 \times 10$ cm^2), using the CC01 detector as a benchmark. By isolating output factors as the only variable configuration parameter in the Eclipse TPS (with consistent PDDs and beam profiles), this work evaluates the feasibility of substituting CC01 data with measurements from clinically available devices for TPS commissioning or QA purposes.

Materials and Methods

Detectors and Output Factor Measurements

This study was designed to evaluate the clinical impact of output factor variations derived from five different radiation detectors with the aim of assessing the feasibility of substituting commonly available clinical detectors for the CC01 detector in small-field dosimetry. The detectors included in the study were the CC01, CC13 ionization chamber, Matrixx Evolution 2D ion chamber array, EPID, and DQA multidetector array. Table 1 summarizes the key technical characteristics of all five detectors used in this study. It includes details such as detector type, active volume, spatial resolution, and material composition, enabling a comparative understanding of their design and functional parameters relevant to small-field dosimetry.

CC01 is an ion chamber detector with an active volume of 0.01 cm^3, widely regarded as a reference standard for small-field output factor measurements because of its minimal volume averaging and high spatial resolution. The CC13, in contrast, is a 0.13 cm^3 cylindrical ionization chamber typically used for standard field dosimetry but is often challenged by volume averaging effects in small fields. The Matrixx Evolution, as shown in Figure 1, is a 2D ionization chamber array comprising 1020 vented ion chambers with an active volume of 0.08 cm3 spaced at 7.62 mm intervals, designed primarily for patient-specific QA, but evaluated here for its performance in field size-specific output measurements. The EPID aS1200 (Varian Medical Systems, Palo Alto, California, USA), shown in Figure 2, is a high-resolution amorphous silicon panel commonly used for portal imaging and in vivo dosimetry. DQA, as shown in Figure 3, is a daily QA device that houses multiple solid-state detectors and is primarily used for linear accelerator performance checks.

All output factor measurements were conducted using a Varian TrueBeam linear accelerator operating at a 6 MV FFF photon energy. The measurements were performed under standard reference conditions. A fixed source-to-surface distance (SSD) of 100 cm was used, and the detectors were placed at a depth of 10 cm within the phantom. Output factors were measured for asymmetric field sizes ranging from 1×1 cm^2 to 10×10 cm^2, in 1 cm increments, totaling 100 measurements

Table 1. **Technical specifications of the detectors (CC01, CC13, Matrixx Evolution, EPID, IBA DQA)**

Specification	IBA CC01	IBA CC13	Varian aS1200 EPID	IBA Matrixx Evolution	IBA DQA
Detector Type	Vented cylindrical ionization chamber	Vented cylindrical ionization chamber	Amorphous silicon (aSi) flat-panel detector	2D array 1020 ion chambers	2D array 125 ion chambers
Sensitive Volume	0.01 cm^3	0.13 cm^3	N/A	0.08 cm^3	0.016 cm^3
Detector Dimensions	Radius: 1.0 mm; Length: 3.6 mm	Radius: 3.0 mm; Length: 5.8 mm	43 × 43 cm^2; Pixel: 0.336 mm	24 × 24 cm^2; Spacing: 7.62 mm	20 × 20 cm^2; Varies by location
Material	PMMA wall with graphite; Al electrode	PMMA wall with graphite; Al electrode	aSi with lead shielding	Air-filled ion chambers	Air-filled ion chambers
Recommended Field Size	≥ 1 × 1 cm^2	≥ 3 × 3 cm^2	≥ 1 × 1 cm^2	≥ 2 × 2 cm^2	≥ 2 × 2 cm^2
Spatial Resolution	Very high	Moderate	High	Low to moderate	Moderate (~5 mm spacing)
Typical Sensitivity	0.5 nC/Gy	3.6 nC/Gy	N/A	N/A	N/A
Polarizing Voltage	± 300 V (max. ± 500 V)	± 300 V (max. ± 500 V)	N/A	N/A	N/A
Leakage Current	≤ 3 fA	≤ 3 fA	N/A	N/A	N/A
Temperature Range	15°C – 35°C	15°C – 35°C	N/A	N/A	N/A
Key Features	High resolution; minimal averaging; ideal for small-field dosimetry	General-purpose; limited for fields <2 × 2 cm^2	High-resolution; integrated calibration and shielding; supports FFF	Quick QA; limited resolution for small fields	Fast setup; real-time output verification

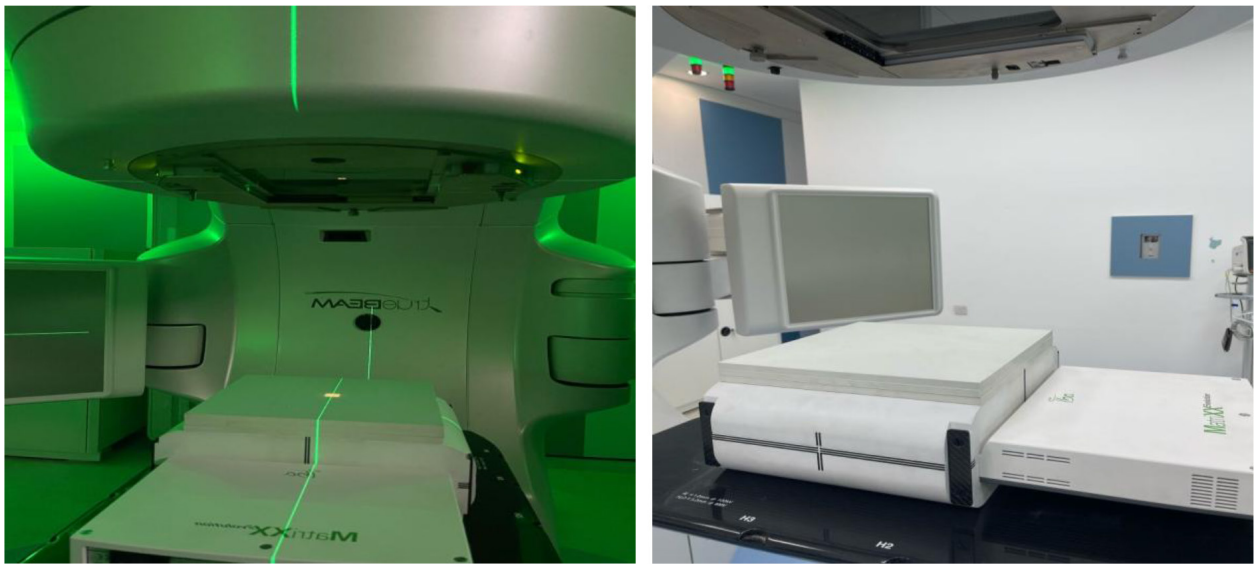

Fig. 1 **The 2D array Matrixx (Evaluation, version 2.15, IBA, Germany).**

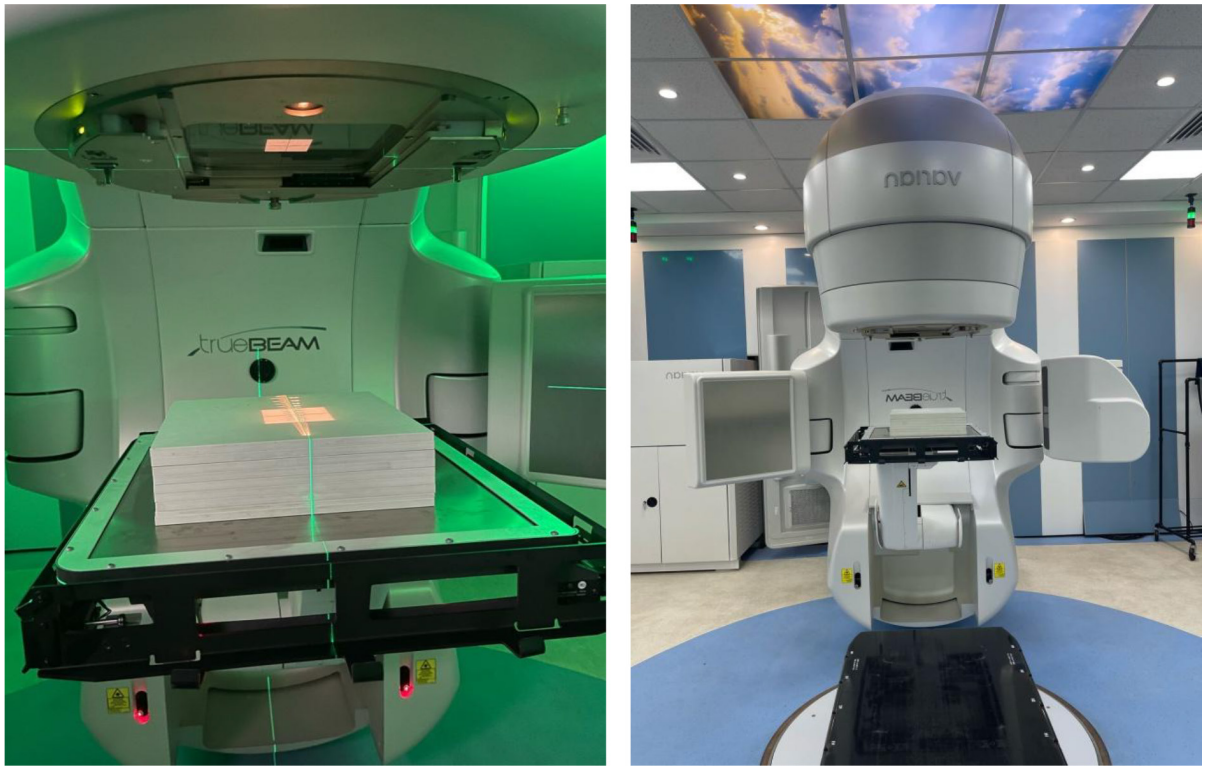

Fig. 2 **The EPID (Varian Medical Systems, version 2.7, Palo Alto, California, USA).**

per detector. Each measurement was normalized to the reading obtained for a 10 × 10 cm² field, which served as the reference field size. All readings were repeated three times and averaged to minimize random errors. The CC01 detector served as the benchmark against which the output factors from the other detectors were compared.

Both the CC01 and CC13 ionization chambers were calibrated and corrected according to the field output correction factors (FOCFs) provided in the IAEA TRS-483 protocol. These detectors served as reference instruments for small-field dosimetry. The MatriXX Evolution, EPID, and DQA detectors were then cross-calibrated against the CC01 and CC13 under identical beam conditions. Although FOCFs were not directly applied to the alternative detectors, this cross-calibration approach enabled consistent output factor measurements across all devices.

Eclipse TPS Configuration and Machine Modeling

To evaluate how detector-specific output factors influence clinical dose calculations, each detector was modeled as a unique virtual linear accelerator within the Eclipse Treatment Planning System (TPS), version 17.0 (Varian Medical Systems, Palo Alto, CA). The beam configuration for each machine was kept identical in all aspects, except for the output factor table, which was customized using the measurements acquired with each respective detector. All other

Fig. 3 **The DQA (IBA, version 2.15, Germany).**

beam modeling parameters, including PDD curves, dose profiles, off-axis ratios, and energy spectra, were held constant across all the machine models. This approach ensured that any variations in the calculated dose distributions could be attributed solely to differences in the output factors. Each machine model was configured using the photon-beam configuration module of Eclipse. Customized output factor data were imported manually for each machine to ensure consistent data formatting and normalization. Following a successful configuration, each machine was subjected to internal TPS consistency checks to validate the integrity of the beam model.

Patient Selection and Treatment Prescription

Twenty patients diagnosed with brain astrocytomas were retrospectively selected for inclusion in the study. All patients had been previously treated and had complete simulation CT datasets, contouring, and planning. The plans were selected to represent a typical clinical population receiving hypofractionated radiotherapy for primary or recurrent astrocytomas. All patients were prescribed a total dose of 30 Gy delivered in five fractions (6 Gy per fraction), consistent with hypofractionated protocols for brain tumors. Target volumes were delineated according to the institutional guidelines. The Gross Tumor Volume was defined based on MRI fusion and contrast enhancement, whereas the Clinical Target Volume (CTV) encompassed a margin for subclinical disease extension. The Planning Target Volume (PTV) was created by expanding the CTV by a uniform 3–5 mm margin to account for setup uncertainty and intra-fraction motion.

Organs-at-risk (OARs), including the brainstem and bilateral cochleae, were contoured based on standardized anatomical landmarks. The cochleae were contoured on axial CT images using bone windows, and the brainstem was delineated from the most inferior to the superior extent. These structures were included in the plan optimization with institutional dose constraints.

Treatment Planning and Dose Recalculation

For each patient, a reference treatment plan was generated using volumetric modulated arc therapy (VMAT) with one full arc and collimator rotation of 0°. The plan was initially created and optimized using a machine configuration corresponding to the CC01 detector. This reference plan was then duplicated for each of the other four machine configurations (CC13, Matrixx Evolution, EPID, and DQA), and the dose was re-optimized and recalculated without any further modification to the beam geometry, weights, or optimization parameters. By recalculating the same optimized plan using different detector-specific output factor data, we isolated and quantified the dosimetric differences introduced solely by variations in the output factor configuration. This method preserves the clinical validity of the original plan and ensures a fair basis for comparison across detector types.

Dosimetric Analysis

The dosimetric parameters for each plan were extracted using the Eclipse dose-volume histogram (DVH) analysis tool. For the PTV, the evaluated metrics included the maximum point dose (D_{max}), dose covering 107% of the PTV volume (D_{107}), and dose covering 95% of the PTV volume (D_{95}). OARs were assessed by analyzing the maximum dose (D_{max}) and the dose to the hottest 0.5 cc volume ($D_{0.5}$cc) for the brainstem, along with the maximum dose to both the ipsilateral and contralateral cochleae. Additionally, treatment efficiency was evaluated based on the total monitor units (MUs) required for plan delivery. These metrics were selected to evaluate both the effectiveness of target coverage and the preservation of OAR dose limits as well as to determine the impact of output factor differences on treatment delivery time and machine workload.

Statistical Evaluation

Statistical analyses were conducted using IBM SPSS Statistics (version 20.0), with the results reported as mean values and

standard deviations. The initial step involved assessing data for normality. When the data met this criterion, parametric repeated-measures ANOVA was employed; otherwise, the nonparametric Friedman test was utilized. A paired test was selected, because the same patients were evaluated for each beam energy. Statistical significance was set at the 95% confidence level.

Results

In this study, we experimentally investigated the dosimetric consequences of configuring small-field output factors in the Eclipse TPS using various clinically available detectors, namely the CC13 ionization chamber, MatriXX Evolution, EPID, and DQA systems, compared with the CC01 ionization chamber detector, which served as the reference standard. Importantly, only the output factor values were varied in the TPS configuration, whereas the PDDs and beam profiles were kept constant. This approach allowed us to isolate the impact of detector-dependent output factor variations on the dosimetric accuracy of the plans, particularly for stereotactic applications where small-field effects are pronounced.

The dosimetric assessment revealed that the D_{max} within the PTV was minimally influenced by the choice of the detector. The CC01 detector reported a mean D_{max} of 108.61% ± 1.45%, while the CC13, MatriXX Evolution, EPID, and DQA yielded values of 108.95% ± 1.39%, 109.12% ± 1.33%, 108.49% ± 1.45%, and 108.84% ± 1.53%, respectively. Although these differences were not statistically significant (*P*-value = 0.10), the MatriXX Evolution exhibited a slight numerical elevation in D_{max}, potentially attributable to its finite detector spacing and volume-averaging effects that may amplify peak dose estimations. In contrast, EPID showed a marginally lower D_{max}, likely owing to its integrated smoothing algorithms and its response characteristics in high-gradient regions, as illustrated in Tables 2 and 3.

The dose that covered 95% of the PTV ($D_{95\%}$) was consistent across the detectors. The Razor detector showed a $D_{95\%}$ of 98.63% ± 1.48%, while CC13, MatriXX Evolution, EPID, and DQA reported 99.15% ± 1.41%, 98.80% ± 1.38%, 98.76% ± 1.45%, and 98.89% ± 1.61%, respectively. These results suggest a negligible impact on PTV coverage, with no statistically significant differences (P = 0.12), reinforcing the robustness of $D_{95\%}$ to small variations in output factors when beam modeling is otherwise identical. The hotspot dose ($D_{107\%}$) within the PTV showed a slightly higher variability. While Razor recorded a mean $D_{107\%}$ volume of 2.08% ± 0.85%, MatriXX Evolution yielded a slightly higher value of 2.24% ± 1.02%, and EPID had the lowest at 1.41% ± 0.71%. CC13 and DQA presented intermediate values of 1.79% ± 0.70% and 1.68% ± 0.73%, respectively. Although these differences were not statistically significant (P = 0.42), the under-response of EPID in capturing small-volume hot spots may be attributed to its detector design and internal processing algorithms, which smoothen out peak intensities. Conversely, the MatriXX Evolution showed a minor trend toward overestimation, likely due to its larger active volume, as shown in Figure 4.

The CI and HI remained largely unaffected by the choice of detectors. The CI values were consistently close to 0.97–0.98 across all configurations (P = 1.000), indicating a stable spatial dose conformation, regardless of the output factor source. Similarly, the homogeneity index hovered around 1.08 for all detectors, with a slight increase to 1.09 in the MatriXX-based configuration, again reflecting the small influence of the variance of the output factor on dose uniformity (P = 0.19). With respect to the spatial dose fall-off, as quantified by the GD, the Razor detector yielded a mean GD of 0.87 cm ± 0.04. The other detectors showed slightly lower GD values, with CC13, MatriXX Evolution, EPID, and DQA reporting 0.83 ± 0.04 cm, 0.83 ± 0.04 cm, 0.85 ± 0.03 cm, and 0.83 ± 0.03 cm, respectively. These results suggest a minimal but observable narrowing of the penumbra region when using alternative detectors, although the differences were not statistically significant (P = 0.27), as demonstrated in Tables 2 and 3.

Table 2. **Mean and standard deviation of dosimetric and treatment delivery parameters for five detectors calculated using the Eclipse TPS**

Parameters		Mean ± SD				
		CC01 (A)	CC13 (B)	MATRIXX (C)	EPID (D)	DailyQA (E)
PTV	D_{max} (%)	108.61 ± 1.45	108.87 ± 1.78	109.12 ± 1.42	108.49 ± 1.64	108.58 ± 1.68
	D_{95} (%)	98.63 ± 1.67	99.15 ± 1.47	99.04 ± 1.58	99.02 ± 1.69	99.14 ± 1.48
	D_{107} (%)	2.08 ± 2.79	1.94 ± 2.29	2.24 ± 2.13	1.41 ± 2.23	1.87 ± 2.34
High and intermediate dose spillages	CI	0.97 ± 0.11	0.97 ± 0.13	0.97 ± 0.11	0.98 ± 0.11	0.97 ± 0.13
	HI	1.08 ± 0.01	1.08 ± 0.02	1.09 ± 0.01	1.08 ± 0.02	1.07 ± 0.01
	GD (cm)	0.87 ± 0.11	0.83 ± 0.06	0.84 ± 0.07	0.83 ± 0.06	0.83 ± 0.06
Brainstem	D_{max} (Gy)	26.28 ± 0.67	26.24 ± 0.44	26.35 ± 0.45	26.37 ± 0.26	26.36 ± 0.39
	D0.5cc (Gy)	22.33 ± 1.19	21.63 ± 1.75	21.44 ± 1.60	21.42 ± 1.68	22.28 ± 0.88
Cochlea	D_{max} (Gy)	21.56 ± 4.85	22.72 ± 5.10	22.19 ± 4.91	21.72 ± 4.98	21.97 ± 5.00
Treatment delivery	MU	1214 ± 199	1197 ± 203	1176 ± 195	1246 ± 195	1202 ± 212

HI: heterogeneity index; CI: conformity index; MU: monitor unit; GD: gradient distance.

Table 3. **Comparison between five detectors measurements in the dosimetric and treatment delivery parametrs using *P*–value analysis**

Parameters		*P*-value			
		A vs B	A vs C	A vs D	A vs E
PTV	D_{max} (%)	0.09	0.10	0.45	0.87
	$D_{95\%}$ (%)	0.28	0.12	0.36	0.20
	$D_{107\%}$ (%)	0.43	0.57	0.54	0.77
High and intermediate dose spillages	CI	1.00	1.00	0.56	1.00
	HI	1.00	0.19	0.28	0.53
	GD (cm)	0.31	0.38	0.27	0.31
Brainstem	D_{max} (Gy)	0.82	0.82	0.61	0.70
	D0. 5cc (Gy)	0.20	0.10	0.09	0.73
Cochlea	D_{max} (Gy)	0.21	0.45	0.82	0.58
Treatment delivery	MU	0.49	0.22	0.13	0.22

HI: heterogeneity index; CI: conformity index; MU: monitor unit; GD: gradient distance.

The dosimetric differences remained small in terms of the OAR sparing. The maximum dose to the brainstem was 26.24 ± 1.52 Gy with the Razor detector and closely mirrored by CC13 (26.30 ± 1.53 Gy), MatriXX Evolution (26.34 ± 1.51 Gy), EPID (26.37 ± 1.50 Gy), and DQA (26.32 ± 1.51 Gy), with a non-significant *P*-value of 0.63. For the brainstem $D_{0.5cc}$, a parameter more sensitive to localized dose differences, Razor recorded 22.33 ± 1.74 Gy, while CC13, MatriXX Evolution, EPID, and DQA produced 21.88 ± 1.91 Gy, 22.05 ± 1.97 Gy, 21.42 ± 1.84 Gy, and 21.66 ± 1.84 Gy, respectively. Although these differences approached statistical significance (P = 0.09), particularly with EPID showing a 0.9 Gy underestimation compared to CC01, they were within clinically acceptable margins. The cochlea D_{max} also showed consistent results, with CC01 reporting 21.56 ± 6.53 Gy and the remaining detectors yielding values within ± 1.2 Gy of this reference: CC13 (22.72 ± 6.42 Gy), MatriXX Evolution (22.03 ± 6.13 Gy), EPID (21.90 ± 6.31 Gy), and DQA (22.21 ± 6.45 Gy), with no significant differences observed (P = 0.49), as represented in Tables 2 and 3.

Finally, an evaluation of the MUs required to achieve equivalent dose distributions across different output factor configurations revealed no statistically significant differences (P = 0.13–0.49). The Razor-based plan required an average of 1214 ± 99 MUs. The MatriXX Evolution required the fewest

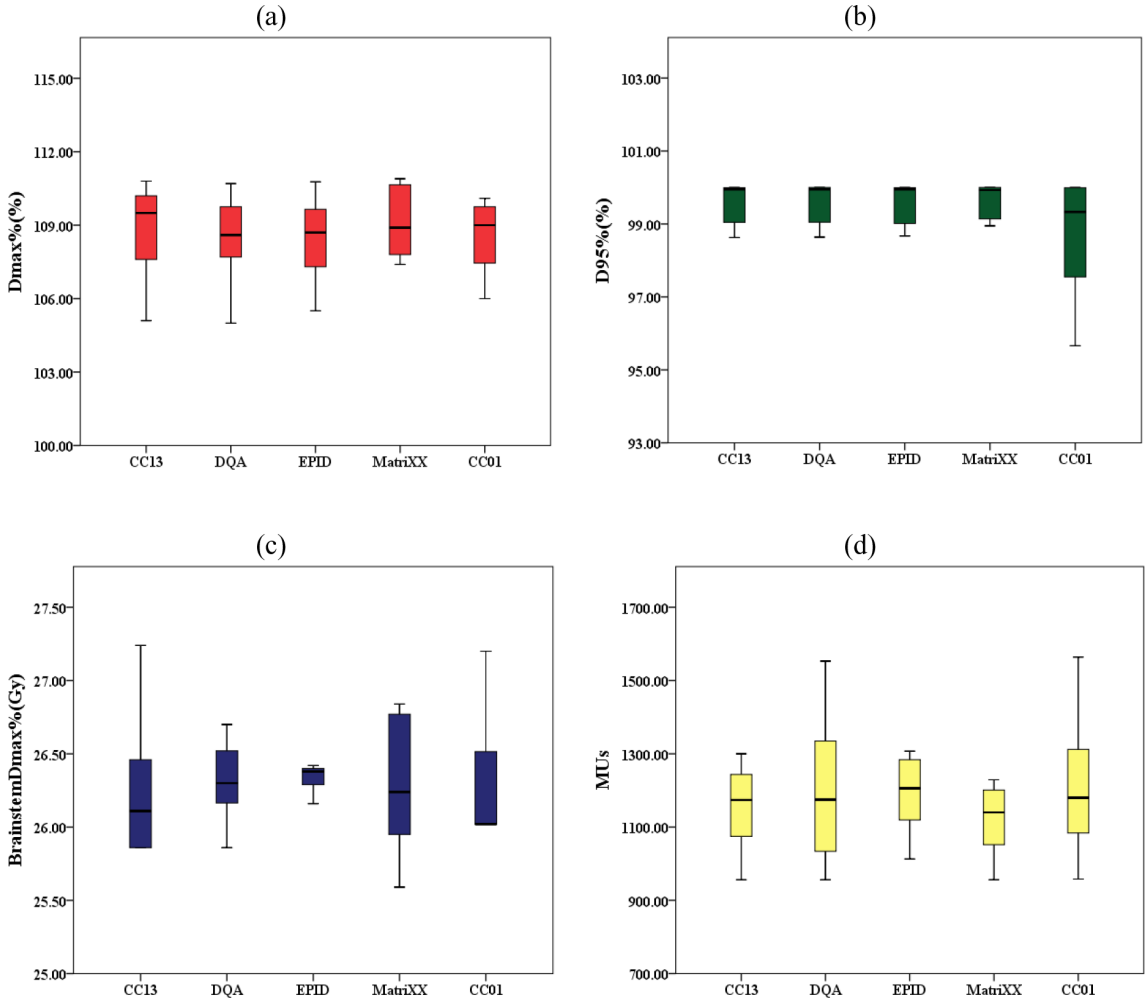

Fig. 4 **Box-whisker plots comparing (a) D_{95} (%) of the PTV, (b) D_{max} (%) of the PTV, (c) D_{max} (%) of the brainstem, and (d) total monitor units (MUs) across plans generated using output factors measured with different detectors: CC01, CC13, MatriXX, EPID, and DQA. Boxes represent the interquartile range, with the horizontal line indicating the median. Whiskers denote the range excluding outliers.**

MUs (1176 ± 93), while EPID-based planning resulted in the highest MU requirement (1246 ± 106), potentially due to subtle underestimation of field output leading to compensatory increases in beam-on time, as shown in Tables 2 and 3.

Discussion

Accurate dosimetry in small radiation fields is challenged by the loss of lateral charged-particle equilibrium, steep dose gradients, and partial occlusion of the primary photon source.[15] This study addressed these challenges by experimentally comparing the dosimetric accuracy of widely available clinical detectors, namely the CC13 ionization chamber, MatriXX Evolution, EPID, and DQA systems, against the CC01 detector, which is recommended by IAEA TRS-483 for small-field dosimetry because of its high spatial resolution and minimal perturbation effects.

Our results confirm that large-volume detectors such as CC13 and Matrixx Evolution overestimate small-field output factors owing to volume averaging and perturbation effects, as documented in earlier literature.[16,17] This did not translate into an increased PTV D_{max}, D_{95}%, and D_{107}% when these detectors were used to configure the Eclipse TPS, potentially leading to overtreatment. From a clinical implementation perspective, the ability to substitute the CC01 detector with more accessible tools such as CC13 or MatriXX is appealing, particularly in settings where specialized small-field detectors are not readily available. The Matrixx Evolution detector, with its 7.62 mm ion chamber spacing and sensitive volume of approximately 0.08 cm^3, tends to average the dose across high gradient regions, leading to inflated output factor values. In contrast, CC13, although relatively smaller than Matrixx Evolution, still lacks the resolution necessary for sub-centimeter fields and has been shown to overestimate doses in several studies when used without appropriate correction factors.[18,19]

The MatriXX Evolution showed good agreement with CC01 for most high-dose parameters and was supported in small-field dosimetry when properly calibrated. The EPID slightly underestimated the dose compared to CC01, although not significantly, with prior studies supporting its use in small-field QA with appropriate calibration. DQA showed excellent agreement with CC01 across all parameters, consistent with previous findings. DQA showed the largest discrepancies and least consistency, which is consistent with its intended use for routine QA rather than dosimetric commissioning. The CI and HI showed no significant differences across detectors, suggesting a stable spatial dose distribution when the PDDs and profiles are constant. However, D_{max}%, D_{107}%, and D_{95}% were more sensitive to OF changes, particularly with EPID and Daily QA, leading to increased MUs during planning. The EPID and Daily QA showed clinically relevant underestimations in PTV coverage parameters, consistent with prior studies citing energy dependence and volume averaging. Increased MUs reflect Eclipse compensation for underestimated OFs, which can impact efficiency and dose accuracy in hypofractionated treatments.[20–25]

Subsequent studies have further examined the performance of CC01, CC13, and diode detectors in small-field dosimetry and their implications for commissioning Eclipse TPS. Notably, Eclipse often excludes OF data for fields smaller than 1 × 1 cm^2, which results in increased uncertainty. A recent investigation revealed MU deviations as high as 6–7.5% when the Eclipse models lacked output data for 1 × 1 cm^2 fields, underscoring the importance of extending the OF table and incorporating measured values. Other studies have explored the performance of CC01, CC13, and diode detectors in small-field dosimetry and their implications for the commissioning of the Eclipse TPS. For example, Eclipse frequently omitted OF data for fields smaller than 1 × 1 cm^2, which can lead to increased uncertainties. A recent study revealed that MU deviations could be as high as 6–7.5% when Eclipse models lacked output data for 1 × 1 cm^2 fields. This finding underscores the need to extend the OF table and incorporate measured values. A study conducted in 2020 revealed that Eclipse's beam models, when commissioned using CC01 and diode detectors, are capable of producing clinically acceptable outcomes for fields as small as 1.5 × 1.5 cm^2. However, it was noted that discrepancies increase for fields smaller than this size.[26–29] To overcome the limitations of single-point detectors, two-dimensional array devices, such as the IBA MatriXX Evolution, are often used for QA purposes. This detector consists of a grid of ion chambers that provide real-time insights into dose distribution. It has shown exceptional performance in standard QA protocols, achieving gamma pass rates of over 97% in various clinical studies. However, concerns have been raised regarding its angular dependence and limited spatial resolution, especially in very small fields. While the IBA MatriXX Evolution is invaluable for standard IMRT QA, its limitations become more pronounced in stereotactic conditions.[30–32]

A key methodological strength of this study was that the consistent PDDs and beam profiles across all detector configurations ensured that any variations in dose distributions were attributable solely to differences in the output factor measurements. This design effectively isolates the influence of each detector on the output factor configuration. Although slight variations were observed in plan quality metrics such as D_{max}%, D_{95}%, and D_{107}%, as well as in OARs doses including D_{max}% and $D_{0.5}$cc% for the brainstem and D_{max}% for the cochlea, and treatment delivery parameters such as MUs, these differences were not clinically significant. These findings support the conclusion that alternative detectors can be reliably used for output-factor commissioning when properly calibrated.

While FOCFs were not explicitly applied to the MatriXX Evolution, EPID, and DQA detectors, it is important to note that the CC01 and CC13 chambers were calibrated and corrected in accordance with the IAEA TRS-483 protocol. These reference detectors were used to cross-calibrate the alternative detectors under the same beam conditions. This approach ensured that all measurements were traceable to detectors corrected with FOCFs. Despite the lack of direct FOCF application for the alternative detectors, their output factor measurements remained within clinically acceptable limits, with no statistically significant deviations observed. These findings support the feasibility of using commonly available clinical detectors as substitutes for the CC01 when proper calibration procedures are followed. These findings support the feasibility of using commonly available clinical detectors for output factor commissioning in stereotactic applications, provided that they are carefully calibrated or validated through collaboration with institutions that have access to CC01 detectors.

Conclusion

Alternative detectors such as the CC13 chamber, MatriXX Evolution, EPID, and DQA can effectively replace the CC01 when appropriate calibration methods are applied to ensure accurate output factor measurements. Radiotherapy centers without access to CC01 detectors should either validate alternative devices or collaborate with other institutions for proper commissioning support. Although different detectors may show slight variations in measured dose metrics, these are generally not statistically significant and remain within clinically acceptable limits. Overall, the CC13, EPID, DQA, and MatriXX Evolution detectors closely align with the Razor detector's dosimetric output, making them suitable alternatives for commissioning output factors in stereotactic applications.

Conflict of Interest

None.

References

1. Das, Indra J., George X. Ding, and Anders Ahnesjö. "Small fields: nonequilibrium radiation dosimetry." Medical Physics 35.1 (2008): 206–215.
2. Alfonso, R., Andreo, P., Capote, R., Huq, M. S., Kilby, W., Kjäll, P., ... & Vatnitsky, S. (2008). A new formalism for reference dosimetry of small and nonstandard fields. Medical Physics, 35(11), 5179–5186.
3. Das, I. J., Francescon, P., Moran, J. M., Ahnesjö, A., Aspradakis, M. M., Cheng, C. W., ... & Sauer, O. A. Final Version: 6/4/21 Report of AAPM Task Group 155: Megavoltage photon beam dosimetry in small fields and non-equilibrium conditions.
4. Palmans, H., Andreo, P., Huq, M. S., Seuntjens, J., Christaki, K. E., & Meghzifene, A. (2018). Dosimetry of small static fields used in external photon beam radiotherapy: summary of TRS-483, the IAEA–AAPM international Code of Practice for reference and relative dose determination. Medical Physics, 45(11), e1123–e1145.
5. Bykova, Y., Khramtsova, N., Shuvaev, I., Zaitseva, N., & Plavnik, R. (2022). Validation of Dosimetric Comissioning Accuracy of IMRT for Versa HD Linear Accelerator with AAPM TG-119 protocol. Meditsinskaya Fizika.
6. Cho, W., Kim, S., Kim, J., Wu, H., Jung, J., Kim, M., Suh, T., Kim, J., & Kim, J. (2015). Dosimetric effects on small-field beam-modeling for stereotactic body radiation therapy. Journal of the Korean Physical Society, 66, 678–693.
7. Li, M., , P., Tian, Y., Miao, J., Men, K., Zhang, K., & Niu, C. (2019). Small field output factor measurement and correction method based on IAEA report No.483. Chinese Journal of Radiation Oncology, 28, 452–456.
8. Nasir, M., Amjad, N., Razzaq, A., & Siddique, T. (2017). Measurement and Analysis of PDDs Profile and Output Factors for Small Field Sizes by cc13 and Micro-Chamber cc01. International Journal of Medical Physics, Clinical Engineering and Radiation Oncology, 06, 36–56.
9. Cho, W., Kim, S., Kim, J., Wu, H., Jung, J., Kim, M., Suh, T., Kim, J., & Kim, J. (2015). Dosimetric effects on small-field beam-modeling for stereotactic body radiation therapy. Journal of the Korean Physical Society, 66, 678–693.
10. Pino, R., Therriault-Proulx, F., Wang, X., Yang, J., & Beddar, S. (2014). SU-E-T-423: TrueBeam Small Field Dosimetry Using Commercial Plastic Scintillation and Other Stereotactic Detectors.. Medical physics, 41 6, 323.
11. Elshamndy, S., Francescon, P., Satariano, N., Orlandi, C., Abouelenein, H., & Ahmed, A. (2019). Comparative Study of Output Factors of Small Field Sizes Dosimetry Systems. The Medical Journal of Cairo University.
12. Behinaein, S., Osei, E., Darko, J., Charland, P., & Bassi, D. (2019). Evaluating small field dosimetry with the Acuros XB (AXB) and analytical anisotropic algorithm (AAA) dose calculation algorithms in the eclipse treatment planning system. Journal of Radiotherapy in Practice, 18, 353–364.
13. Francescon, P., Kilby, W., Satariano, N., & Cora, S. (2012). Monte Carlo simulated correction factors for machine specific reference field dose calibration and output factor measurement using fixed and iris collimators on the CyberKnife system. Physics in Medicine & Biology, 57(12), 3741.
14. Bassinet, C., Huet, C., Derreumaux, S., Brunet, G., Chéa, M., Baumann, M., ... & Clairand, I. (2013). Small fields output factors measurements and correction factors determination for several detectors for a CyberKnife® and linear accelerators equipped with microMLC and circular cones. Medical physics, 40(7), 071725.
15. Sresty, N. M., Raju, A. K., Kumar, T. A., Ahmed, S., & Ahmed, Y. (2018). Poster. Journal of Medical Physics, 43(Suppl 1), S39–S111.
16. Sauer, O. A., & Wilbert, J. (2007). Measurement of output factors for small photon beams. Medical physics, 34(6Part1), 1983–1988.
17. Aspradakis, M. M., Byrne, J. P., Palmans, H., Duane, S., Conway, J., Warrington, A. P., & Rosser, K. (2010). IPEM Report 103: Small field MV photon dosimetry (No. IAEA-CN--182).
18. Nainggolan, A., & Pawiro, S. A. (2019). Dosimetric evaluation of volumetric modulated arc therapy (VMAT) and intensity modulated radiotherapy (IMRT) using AAPM TG 119 protocol. Journal of Biomedical Physics & Engineering, 9(4), 395.
19. Bhardwaj, B. C., Trivedi, G., Prasher, S., & Kumar, M. (2020, May). Commissioning of Clinac IX Trilogy Linear Accelerator for Stereotactic Radiosurgery. In Journal of Physics: Conference Series (Vol. 1531, No. 1, p. 012032). IOP Publishing.
20. Raoui, Y., Herrassi, Y., Elouardy, K., Sebihi, R., Ayad, M., & Vp, P. (2021). Beam modeling in commercial treatment planning system for IMRT and VMAT performance with an Elekta MLCI 2 multileaf collimator. Iran J Med Phys, 18, 452–60.
21. Ritter, T. A., Gallagher, I., & Roberson, P. L. (2014). Using a 2D detector array for meaningful and efficient linear accelerator beam property validations. Journal of Applied Clinical Medical Physics, 15(6), 46–58.
22. McCurdy, B. M. C., & Greer, P. B. (2009). Dosimetric properties of an amorphous-silicon EPID used in continuous acquisition mode for application to dynamic and arc IMRT. Medical physics, 36(7), 3028–3039.
23. Van Elmpt, W., McDermott, L., Nijsten, S., Wendling, M., Lambin, P., & Mijnheer, B. (2008). A literature review of electronic portal imaging for radiotherapy dosimetry. Radiotherapy and oncology, 88(3), 289–309.
24. Winkler, P., Hefner, A., & Georg, D. (2005). Dose-response characteristics of an amorphous silicon EPID. Medical physics, 32(10), 3095–3105.
25. Greer, P. B., & Popescu, C. C. (2003). Dosimetric properties of an amorphous silicon electronic portal imaging device for verification of dynamic intensity modulated radiation therapy. Medical physics, 30(7), 1618–1627.
26. Zaila, A., Adili, M., & Bamajboor, S. (2016). Pylinac: A toolkit for performing TG-142 QA related tasks on linear accelerator. Physica Medica, 32, 292–293.
27. Wu, N. (2022). Extending the EclipseTM AcurosXB output factor table for small field radiosurgery. Journal of Applied Clinical Medical Physics, 24.
28. Kinhikar, R., Saini, V., Upreti, R., Kale, S., Sutar, A., Tambe, C., & Kadam, S. (2020). Measurement of the small field output factors for 10 MV photon beam using IAEA TRS-483 dosimetry protocol and implementation in Eclipse TPS commissioning. Biomedical Physics & Engineering Express, 6.
29. Dorenlot, A., Hoog, C., Tessonnier, T., Nomikossoff, N., Benkreira, M., & Portal, T. (2013). Retrospective of 300 delivery quality assurance of patients treated with the tomotherapy HI-ART 2 using the IBA matrixx-evolution. Physica Medica, 29.
30. Wolfsberger, L., Wagar, M., Nitsch, P., Bhagwat, M., & Zygmanski, P. (2010). Angular dose dependency of MatriXX TM and its calibration. Journal of Applied Clinical Medical Physics, 11, 241–251.
31. Xing, A., Arumugam, S., Deshpande, S., George, A., Holloway, L., Vial, P., & Goozée, G. (2014). SU-E-T-407: Evaluation of Four Commercial Dosimetry Systems for Routine Patient-Specific Tomotherapy Delivery Quality Assurance. Medical physics, 41 6, 319.
32. Alnidawi, I. H., Yaseen, M. N., Khalil, M. M., & Ammar, H. M. (2022). Evaluating the performance of two matched elekta versa HD machines for agility MLC modeling in VMAT plans using the monaco treatment planning system. Onkologia i Radioterapia, 16(1).